Applied Physics Letters

RESEARCH ARTICLE | FEBRUARY 27 2024

Single-photon emission from silicon-vacancy color centers in polycrystalline diamond membranes

Assegid Mengistu Flatae ; Florian Sledz ; Haritha Kambalathmana; Stefano Lagomarsino; Hongcai Wang; Nicla Gelli ; Silvio Sciortino; Eckhard Wörner; Christoph Wild; Benjamin Butz; Mario Agio

Appl. Phys. Lett. 124, 094001 (2024)
https://doi.org/10.1063/5.0191665

AIP Publishing

Applied Physics Letters ARTICLE pubs.aip.org/aip/apl

Single-photon emission from silicon-vacancy color centers in polycrystalline diamond membranes

Cite as: Appl. Phys. Lett. **124**, 094001 (2024); doi: 10.1063/5.0191665
Submitted: 15 December 2023 · Accepted: 9 February 2024 ·
Published Online: 27 February 2024

Assegid Mengistu Flatae,[1,2,a] Florian Sledz,[1,2] Haritha Kambalathmana,[1,2] Stefano Lagomarsino,[3] Hongcai Wang,[2,4,5] Nicla Gelli,[3] Silvio Sciortino,[3,6,7] Eckhard Wörner,[8] Christoph Wild,[8] Benjamin Butz,[2,4] and Mario Agio[1,2,7]

AFFILIATIONS

[1]Laboratory of Nano-Optics, University of Siegen, 57072 Siegen, Germany
[2]Cμ-Research Center of Micro- and Nanochemistry and (Bio)Technology, University of Siegen, 57068 Siegen, Germany
[3]Istituto Nazionale di Fisica Nucleare, Sezione di Firenze, 50019 Sesto Fiorentino, Italy
[4]Micro- and Nanoanalytics Group, University of Siegen, 57076 Siegen, Germany
[5]Institute for Materials, Ruhr-University Bochum, 44801 Bochum, Germany
[6]Department of Physics and Astronomy, University of Florence, 50019 Sesto Fiorentino, Italy
[7]National Institute of Optics (INO), National Research Council (CNR), 50125 Florence, Italy
[8]Diamond Materials GmbH, 79108 Freiburg, Germany

[a)]**Author to whom correspondence should be addressed:** assegid.flatae@uni-siegen.de

ABSTRACT

Single-color centers in thin polycrystalline diamond membranes allow the platform to be used in integrated quantum photonics, hybrid quantum systems, and other complex functional materials. While single-crystal diamond membranes are still technologically challenging to fabricate as they cannot be grown on a non-diamond substrate, free-standing polycrystalline diamond membranes can be conveniently fabricated at large-scale from nanocrystalline diamond seeds on a substrate that can be selectively etched. However, their practical application for quantum photonics is so far limited by crystallographic defects, impurities, graphitic grain boundaries, small grain sizes, scattering loss, and strain. In this paper, we report on a single-photon source based on silicon-vacancy color centers in a polycrystalline diamond membrane. We discuss the spectroscopic approach and quantify the photon statistics, obtaining a $g^2(0) \approx 0.04$. Our findings hold promise for introducing polycrystalline diamond to quantum photonics and hybrid quantum systems.

Color centers in diamonds are developed into quantum devices as reliable single-photon sources,[1] for quantum computers and networks[2,3] and as quantum sensors.[4] Particularly, the negatively charged silicon-vacancy (SiV^-) color center has been identified as a promising single-photon source as it exhibits strong emission in the zero-phonon line (ZPL) of around 738 nm, with an excited-state lifetime of about 1 ns (Refs. 5 and 6) and operation both at room and higher temperatures.[7] Single-photon rates in the range of megahertz and the nature of its polarized emission[8] also indicate potential application for instance in quantum cryptography[9] and quantum frequency conversion.[10] For robust heterostructure devices, integrated quantum photonics, hybrid quantum systems,[11] and other complex functional materials, the color centers should be in thin free-standing membranes of thickness from a few micrometers to a hundred nanometers. It is straightforward to think of using the highest-quality single-crystal diamond. However, the fabrication of single-crystal diamond membranes is technologically challenging as they cannot be grown on a non-diamond substrate, their physical and chemical properties also make the micro/nanostructuring far behind advanced material platforms like silicon technology.[11–15] On the other hand, free-standing polycrystalline diamond membranes can be easily obtained from nanocrystalline diamond seeds supported by a substrate that can be selectively (wet-)etched.[16,17] However, their practical application for quantum optics or integrated quantum photonics is so far limited due to crystallographic defects mainly of the non-diamond carbon phases of the host matrix.[17–19] Particularly, the sp^2 carbon hybridized part of grain center and

boundaries deteriorates the quantum efficiency of the emitter,[5,11,19] and the background photoluminescence prevents addressing single-color centers in polycrystalline membranes.[20]

In this paper, we report on the observation of a single-photon source based on a SiV color center in a polycrystalline diamond membrane. We discuss the spectroscopic approach and quantify the photon statistics.

At first, different diamond films with thicknesses of 55 nm, 100 nm, 170 nm, 370 nm, 3 μm, and 5 μm are fabricated using the microwave plasma chemical vapor deposition (MPCVD) technique on a silicon wafer using a CH_4/H_2 gas mixture, at a substrate temperature of 800 °C, with pressure of 150 mbar and a flow rate of 300 sccm. The concentration of CH_4 is 1%.

After growth, the diamond film is polished, and the 2 mm diameter of the substrate is etched using deep reactive-ion etching, leading to a self-standing membrane on a silicon substrate. In addition, a circular groove of nearly 5 mm in diameter is made around the self-standing membrane. Laser cutting along this groove results in a 5 mm sample with a 2 mm self-standing diamond membrane supported by a silicon frame.

In the fabricated sample, silicon impurities are already present due to diffusion of the atoms from the silicon substrate and/or from the silica reactor windows.[20] We observe that the color centers created using this method form SiV clustering near and at the grain boundary (see the supplementary material, Fig. S1). To create single-color centers in the grain center, rich in sp^3 hybridized carbon phase, we used ion implantation. The Si-ion implantation uses a 3 MV Tandetron accelerator equipped with a HVEE860 negative sputter ion source to accelerate ion species (Si^+, Si^{2+}, Si^{3+}).[21] We implant Si^{3+} ions accelerated at 9 MeV with a fluence of 10^8 cm^{-2}. This fluence is chosen as it allows us to find single emitters in the optical diffraction limit region. Moreover, the implantation depth was controlled by degrading the ion energy further down to a few tens of kilo electron volts using double 2.3 μm thick aluminum foils.

Thermal annealing at 1150 °C for 1 h, with a heating ramp of 20 °C/min, in high vacuum conditions leads to active SiV color centers in the diamond membranes. Annealing allows the implanted impurity atoms to be placed at the lattice positions, makes vacancies mobile, and brings them to the Si atoms. In addition, it reduces the crystal damage, hence minimizing non-radiative recombination caused by the ion implantation, and restores the crystal lattice.[6] After fabrication, the samples are cleaned in a UV-ozone cleaner for 2 h and ultrasonicated with 50% acetone/50% isopropyl alcohol for 2 h and further dried with clean-dry air.

As shown in Fig. 1 schematically and using scanning transmission electron microscopy (STEM) images of a 5 μm thick diamond membrane, the first few hundreds of nanometers are mainly dominated by seed and intermediate layers. These are known to contain high concentrations of sp^2 graphitic carbon and other impurities.[22] The STEM images were acquired using a Thermo Fisher FEI Talos F200X operating at 200 kV. The TEM lamella was prepared by an FEI Helios G4 CX focused ion beam following a standard lift-out procedure and thinned down to about 100 nm with parameters provided in the supplementary material. It is evident that large grains are already observed after a few hundreds of nanometers from the formation of an initial nucleation layer. Bright-field and dark-field STEM images (see also Fig. S2) show that grain sizes larger than the optical diffraction limit can be obtained after a growth of a few micrometers (roughly above 2–3 μm).

Raman and photoluminescence spectroscopy using a confocal μ-photoluminescence optical setup also verifies that the optical properties of the diamond needed for single-photon emission can be obtained

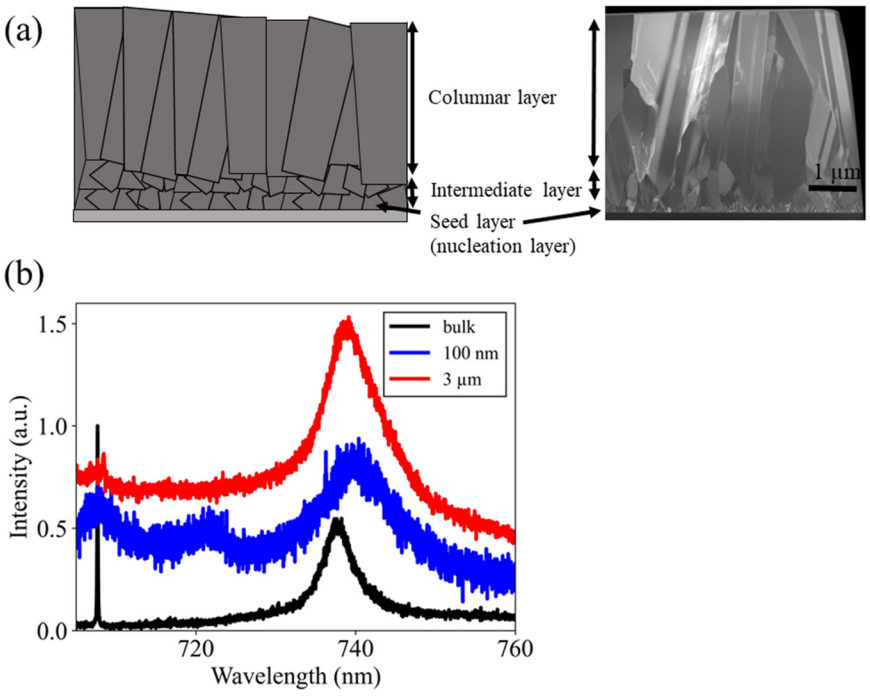

FIG. 1. (a) Schematics and STEM images showing the different layers of a 5 μm thick polycrystalline diamond membrane. (b) Raman and photoluminescence spectrum of a 100 nm thick, 3 μm thick, and bulk-polycrystalline diamond.

for a micrometer-scale thick polycrystalline membrane. Figure 1(b) shows the spectrum of 100 nm thick, 3 μm thick, and bulk polycrystalline diamond excited by 647 nm laser (Coherent, Innova 70, Ar/Kr ion hybrid). The first spectral peak around 708.7 nm of the 100 nm thick diamond corresponds to the 1346 cm^{-1} D band of graphite, partly coinciding with the diamond Raman peak at 708 nm (1332 cm^{-1}) and the one at 720 nm corresponds to the G peak of graphite (1575 cm^{-1}). The peak at 742 nm is attributed to SiV color centers. The strain in the diamond thin film, due to growth on a substrate with a different thermal expansion coefficient,[23] is responsible for the shift in the ZPL of the color centers in the membranes as compared to the typical ZPL at 738 nm of SiV color centers in bulk diamond.[24] The GR1 (single vacancy) color center has also the ZPL at 742 nm, but these defect centers are usually removed when the sample is annealed above 600 °C.[25] As evident from the spectral signatures, the nanodiamond membranes are mainly dominated by the graphitic phase. The photoluminescence spectra of 55, 170, and 370 nm thick diamond membranes show similar optical properties [see the supplementary material, Fig. S3(a)]. The excited-state lifetime measurements of ensembles of color centers in these membranes exhibit a lifetime between 0.5 and 0.8 ns, suggesting an increase in non-radiative decay processes. This is expected as high concentrations of grain boundaries are within the confocal volume. For a diamond membrane thicker than 3 μm, the typical diamond Raman peak appears at 708 nm (1332 cm^{-1}) as shown in Fig. 1(c) (red). Their grain size can also reach a size above a micrometer.[20] Hence, we focus our attention on a 5 μm thick diamond membrane to interrogate single SiV color centers in the grain center.

Optical spectroscopy study of single SiV color centers in the implanted diamond membranes was also performed using the same home-built confocal microscopy along with widefield imaging technique.[26] For effectively suppressing the background due to nitrogen vacancy and other complexes, we used a 690 nm laser [see the supplementary material and Fig. S3(b)].

Figure 2 (blue circle) shows a SiV in the grain center in the spectral region defined by a bandpass filter centered at 740 nm with 13 nm bandwidth (see also Fig. S4). The spectrum of the color center in this grain center exhibits a Lorentzian-like emission profile with the central peak of around 741 nm and a linewidth of 11 nm. The color centers in and near the grain boundaries have a background contribution, and a background corrected Lorentzian fit reveals a linewidth of around 13 nm [see Fig. 2(b)]; a wider spectral window is chosen using a bandpass filter centered at 747 nm with 33 nm bandwidth to observe the spectral trend in more detail. The broadening of the ZPL emission of the color centers in the diamond membrane as compared to bulk is mainly attributed to stress and crystal imperfections. The phonon density of states of an imperfect crystal determines the extent to which the electronic transition interacts with different lattice modes.[27] Stress is also a known source of spectral broadening and shifting of the ZPL of the SiV color center in the diamond membrane.[2,28]

The broad background signal observed in and near the grain boundaries is mainly attributed to sp^2 hybridized and bonded disordered carbon, as it introduces electronic states into the bandgap[29] and to the typical luminescence of the grain boundaries in the polycrystalline diamond.[30]

Time resolved spectroscopy shows the color center in the grain center exhibits a deconvoluted excited-state lifetime of 1.1 ns, as depicted in Fig. 3(a). This value is similar to the lifetime as SiV color centers in the bulk diamond.

Using the Hanbury Brown–Twiss (HBT) intensity interferometry, the second order correlation measurements reveal photon antibunching with $g^2(0) \approx 0.04$ under continuous-wave excitation, verifying the detection of single SiV in the grain center [Fig. 3(b)]. For a pump power below saturation, the color center shows a two-level-type photodynamics as discussed in the supplementary material (see Figs. S5 and S6). However, above saturation, a photon bunching behavior is apparent at a longer delay times, and a three-level scheme is considered to include a shelving state to determine the transition rates (see the discussion in the supplementary material and Fig. S7). Taking into account the linear dependence of the transition rate from the ground state to the excited state γ_{12}, with the excitation power P, and the dependence of the bunching parameters on the excitation power, the excited state decay rate amounts to $\gamma_{21} \approx 909$ MHz, and the transition from the excited state to shelving state becomes $\gamma_{23} \approx 0.714$ MHz, and the de-shelving rate is approximated by $\gamma_{31} \approx 0.7$ MHz (see the supplementary material for detail). Similar values have been reported for single SiV color centers in diamond nanocrystals.[5] The single-photon emission purity of SiV color centers away from the grain center is deteriorated due to the unwanted background and lower crystal quality due to high concentration of sp^2 phases [see Fig. 2(b) black curve and Fig. S8].

One of the important figures of merit for a single-photon source is the photon count rate at saturation and the quantum efficiency of the emitter. Figure 3(c) shows the saturation curve for a single SiV color center. The count rate I has been fitted using the function

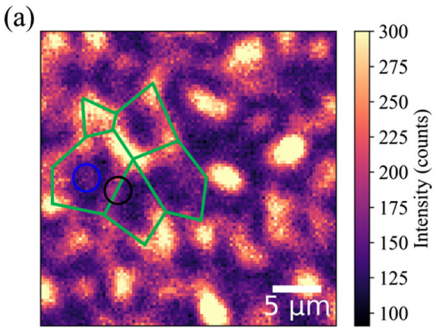

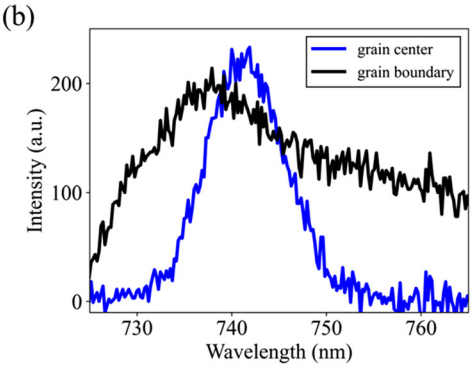

FIG. 2. (a) Widefield image of SiV color centers in a polycrystalline diamond membrane of 5 μm thickness. The green lines show the grain boundaries. The blue and black circles depict SiV color centers inside and on the grain boundaries, respectively. (b) The color center inside the grain boundary [blue circle in (a)] shows a Lorentzian-type emission spectrum (blue curve), while the color centers around the grain boundary [black circle in (a)] have a background contribution (black curve).

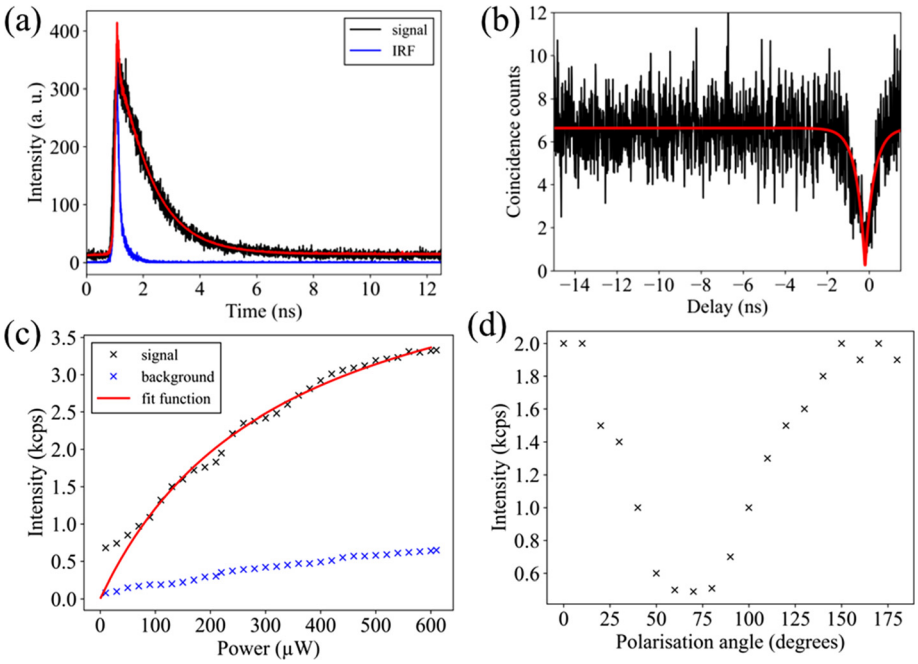

FIG. 3. (a) SiV color center inside the grain center exhibits the excited-state lifetime of around 1.1 ns. The decay curve is deconvoluted from the instrument response function (IRF) (blue curve). (b) Intensity auto-correlation (g^2) measurement using HBT interferometry reveals photon antibunching with $g^2(0) \approx 0.04$. (c) Saturation (black) vs background (blue) as a function of excitation power. (d). Polarization-dependent count rates. The excitation power is kept constant, but the polarization state is changed. The spectra are measured from the 5 μm thick diamond membrane.

$I = \frac{I_\infty}{1+\frac{P_{sat}}{P}} + C_{bg}P$, where P_{sat} is the excitation power at saturation, and I_∞ is the maximum photon count rate (in units of photon counts per second, cps). The background is measured in the nearby region, where no SiV is detected. Using this equation, we found a maximum photon count rate of $I_\infty = 5.2 \times 10^3$ cps (at $P_{sat} = 333\ \mu$W), which corresponds to about $\sim 6 \times 10^5$ cps, taking into account light trapping in the diamond and the overall detection efficiency of our setup.

The experimental determination of the intrinsic quantum efficiency η requires information about radiative and total decay rates. Under low pump power, fluorescence lifetime measurements can be best approximated as the inverse of total decay rates. The determination of radiative decay rates should be carefully considered as transitions from the excited state to the shelving state and back to the ground state take a few hundreds of nanoseconds. In experimental terms, we define the intrinsic quantum efficiency η as the ratio of the number of emitted photons to the number of successful excitations. To determine these two parameters, we saturate a single SiV color center using 1 MHz laser, <90 ps pulse width at FWHM (PicoQuant, PDL 800-D, LDH-D-C-660). The 1 μs pulse separation ensures that each incident laser pulse leads to an excitation, as each of the pulses finds the color center in the ground state after the previous excitation (as shown schematically in Fig. S9). In other words, the number of excitations per second is exactly the same as the repetition rate of the excitation laser. Taking into account the system detection efficiency and light outcoupling efficiency from the host medium, we determine that the total emitted photons per second corresponds to 2.8×10^4 cps. Hence, the intrinsic quantum efficiency is around 2.8%, similar to the quantum efficiency of single SiV color centers in diamond nanocrystals.[5] The radiative- and non-radiative decay rates then will approximately be 26 and 883 MHz, respectively (see the supplementary material for detail).

Another important aspect of the single-photon emission from SiV color centers in diamonds is its ability to emit polarized photons. Many applications, such as quantum cryptography (BB84 protocol), require a well-defined state of polarization.[9] In addition, it allows us to maximize the signal-to-noise ratio as the dipole preferentially absorbs a certain polarization. To measure the polarization contrast visibility, a half-wave plate is used to rotate the angle of polarization of the excitation laser light. Figure 3(d) displays the observed emission of SiV color center for a given polarization angle. The power of the excitation laser is the same for all degrees of polarizations. Polarization contrast visibility of more than 0.85 (85%) is obtained according to $V = \frac{(I_{max}-I_{min})}{I_{max}+I_{min}}$. The deviation from unity (100%) is attributed to an off-plane angular misalignment of the transition dipole moment, depolarization due to the used dichroic mirror, and the multiple- and large angle refraction of the high numerical aperture (NA) objective (NA = 0.95, 50×).

In conclusion, we have reported the single-photon emission from SiV color centers in polycrystalline diamond membranes and discuss the spectroscopic approach to quantify the single-photon emission dynamics. The platform can also be back-etched and/or nanostructured for integrated quantum photonics.[11] In addition, the film thickness allows us to control and manipulate the photophysics using resonant structures, for example, by using planar antennas to achieve large collection efficiency and directionality.[31,32] Furthermore, the proposed approach is general, and it can also be used for other types of color centers, for example, NV and group IV defect centers (such as GeV^-, SnV^-, and PbV^-).

See the supplementary material for further details on the photophysics of SiV color centers in polycrystalline diamond membranes.

The authors gratefully acknowledge financial support from the University of Siegen and the German Research Foundation (DFG) (INST 221/118-1 FUGG, 410405168). A.M.F. would like to thank F. Tantussi and F. De Angelis from the Italian Institute of Technology, Genoa, for instrumentation. B.B. and H.W. acknowledge the access to

the infrastructure of MNaF (Talso F200X TEM) at the University of Siegen and ZGH (Helios G4 CX FIB) at the Ruhr University Bochum.

AUTHOR DECLARATIONS

Conflict of Interest

The authors have no conflicts to disclose.

Author Contributions

Assegid Mengistu Flatae: Conceptualization (lead); Formal analysis (lead); Investigation (lead); Writing – original draft (lead). **Florian Sledz:** Investigation (supporting). **Haritha Kambalathmana:** Investigation (supporting). **Stefano Lagomarsino:** Investigation (supporting). **Hongcai Wang:** Investigation (supporting). **Nicla Gelli:** Investigation (supporting). **Silvio Sciortino:** Investigation (supporting). **Eckhard Wörner:** Methodology (supporting); Resources (supporting). **Christoph Wild:** Methodology (supporting); Resources (supporting). **Benjamin Butz:** Funding acquisition (supporting); Resources (supporting). **Mario Agio:** Conceptualization (lead); Funding acquisition (lead); Investigation (lead); Supervision (lead); Writing – review & editing (lead).

DATA AVAILABILITY

The data that support the findings of this study are available from the corresponding author upon reasonable request.

REFERENCES

[1]I. Aharonovich, S. Castelletto, D. A. Simpson, C.-H. Su, A. D. Greentree, and S. Prawer, "Diamond-based single-photon emitters," Rep. Prog. Phys. **74**(7), 076501 (2011).
[2]S. Pezzagna and J. Meijer, "Quantum computer based on color centers in diamond," Appl. Phys. Rev. **8**(1), 011308 (2021).
[3]M. Ruf, N. H. Wan, H. Choi, D. Englund, and R. Hanson, "Quantum networks based on color centers in diamond," J. Appl. Phys. **130**(7), 070901 (2021).
[4]J. F. Barry, J. M. Schloss, E. Bauch, M. J. Turner, C. A. Hart, L. M. Pham, and R. L. Walsworth, "Sensitivity optimization for NV-diamond magnetometry," Rev. Mod. Phys. **92**(1), 015004 (2020).
[5]E. Neu, M. Agio, and C. Becher, "Photophysics of single silicon vacancy centers in diamond: Implications for single photon emission," Opt. Express **20**(18), 19956 (2012).
[6]S. Lagomarsino, A. M. Flatae, S. Sciortino, F. Gorelli, M. Santoro, F. Tantussi, F. De Angelis, N. Gelli, F. Taccetti, L. Giuntini, and M. Agio, "Optical properties of silicon-vacancy color centers in diamond created by ion implantation and post-annealing," Diamond Relat. Mater. **84**, 196–203 (2018).
[7]S. Lagomarsino, F. Gorelli, M. Santoro, N. Fabbri, A. Hajeb, S. Sciortino, L. Palla, C. Czelusniak, M. Massi, F. Taccetti, L. Giuntini, N. Gelli, D. Y. Fedyanin, F. S. Cataliotti, C. Toninelli, and M. Agio, "Robust luminescence of the silicon-vacancy center in diamond at high temperatures," AIP Adv. **5**(12), 127117 (2015).
[8]E. Neu, M. Fischer, S. Gsell, M. Schreck, and C. Becher, "Fluorescence and polarization spectroscopy of single silicon vacancy centers in heteroepitaxial nanodiamonds on iridium," Phys. Rev. B **84**(20), 205211 (2011).
[9]A. Muller, J. Breguet, and N. Gisin, "Experimental demonstration of quantum cryptography using polarized photons in optical fibre over more than 1 km," Europhys. Lett. **23**(6), 383–388 (1993).
[10]S. Zaske, A. Lenhard, and C. Becher, "Efficient frequency downconversion at the single photon level from the red spectral range to the telecommunications C-band," Opt. Express **19**(13), 12825 (2011).
[11]I. Aharonovich and E. Neu, "Diamond nanophotonics," Adv. Opt. Mater. **2**(10), 911–928 (2014).
[12]A. A. Martin, S. Randolph, A. Botman, M. Toth, and I. Aharonovich, "Maskless milling of diamond by a focused oxygen ion beam," Sci. Rep. **5**(1), 8958 (2015).
[13]B. A. Fairchild, P. Olivero, S. Rubanov, A. D. Greentree, F. Waldermann, R. A. Taylor, I. Walmsley, J. M. Smith, S. Huntington, B. C. Gibson, D. N. Jamieson, and S. Prawer, "Fabrication of ultrathin single-crystal diamond membranes," Adv. Mater. **20**(24), 4793–4798 (2008).
[14]M. P. Hiscocks, K. Ganesan, B. C. Gibson, S. T. Huntington, F. Ladouceur, and S. Prawer, "Diamond waveguides fabricated by reactive ion etching," Opt. Express **16**(24), 19512 (2008).
[15]A. H. Piracha, K. Ganesan, D. W. M. Lau, A. Stacey, L. P. McGuinness, S. Tomljenovic-Hanic, and S. Prawer, "Scalable fabrication of high-quality, ultra-thin single crystal diamond membrane windows," Nanoscale **8**(12), 6860–6865 (2016).
[16]L. Schäfer, A. Bluhm, C.-P. Klages, B. Löchel, L.-M. Buchmann, and H.-L. Huber, "Diamond membranes with controlled stress for submicron lithography," Diamond Relat. Mater. **2**(8), 1191–1196 (1993).
[17]M. Zukerstein, F. Trojánek, P. Koutenský, M. Varga, A. Kromka, M. Kozák, and P. Malý, "Sub-picosecond electron dynamics in polycrystalline diamond films," Diamond Relat. Mater. **108**, 107935 (2020).
[18]P. Galář, B. Dzurňák, M. Varga, M. Marton, A. Kromka, and P. Malý, "Influence of non-diamond carbon phase on recombination mechanisms of photoexcited charge carriers in microcrystalline and nanocrystalline diamond studied by time resolved photoluminescence spectroscopy," Opt. Mater. Express **4**(4), 624 (2014).
[19]F. Trojánek, K. Hamráček, M. Hanák, M. Varga, A. Kromka, O. Babčenko, L. Ondič, and P. Malý, "Light emission dynamics of silicon vacancy centers in a polycrystalline diamond thin film," Nanoscale **15**(6), 2734–2738 (2023).
[20]H. Kambalathmana, A. M. Flatae, L. Hunold, F. Sledz, J. Müller, M. Hepp, P. Schmuki, M. S. Killian, S. Lagomarsino, N. Gelli, S. Sciortino, L. Giuntini, E. Wörner, C. Wild, B. Butz, and M. Agio, "Optical properties of silicon-implanted polycrystalline diamond membranes," Carbon **174**, 295–304 (2021).
[21]S. Lagomarsino, S. Sciortino, N. Gelli, A. M. Flatae, F. Gorelli, M. Santoro, M. Chiari, C. Czelusniac, M. Massi, F. Taccetti, M. Agio, and L. Giuntini, "The center for production of single-photon emitters at the electrostatic-deflector line of the tandem accelerator of LABEC (florence)," Nucl. Instrum. Methods Phys. Res., Sect. B **422**, 31–40 (2018).
[22]C. Dawedeit, S. O. Kucheyev, S. J. Shin, T. M. Willey, M. Bagge-Hansen, T. Braun, Y. M. Wang, B. S. El-Dasher, N. E. Teslich, M. M. Biener, J. Ye, L. Kirste, C.-C. Roehlig, M. Wolfer, E. Woerner, A. W. Van Buuren, A. V. Hamza, C. Wild, and J. Biener, "Grain Size dependent physical and chemical properties of thick CVD diamond films for high energy density physics experiments," Diamond Relat. Mater. **40**, 75–81 (2013).
[23]V. Jirásek, T. Ižák, M. Varga, O. Babchenko, and A. Kromka, "Investigation of residual stress in structured diamond films grown on silicon," Thin Solid Films **589**, 857–863 (2015).
[24]T. Müller, C. Hepp, B. Pingault, E. Neu, S. Gsell, M. Schreck, H. Sternschulte, D. Steinmüller-Nethl, C. Becher, and M. Atatüre, "Optical signatures of silicon-vacancy spins in diamond," Nat. Commun. **5**(1), 3328 (2014).
[25]S. Pezzagna, D. Rogalla, D. Wildanger, J. Meijer, and A. Zaitsev, "Creation and nature of optical centres in diamond for single-photon emission—Overview and critical remarks," New J. Phys. **13**(3), 035024 (2011).
[26]A. M. Flatae, S. Lagomarsino, F. Sledz, N. Soltani, S. S. Nicley, K. Haenen, R. Rechenberg, M. F. Becker, S. Sciortino, N. Gelli, L. Giuntini, F. Taccetti, and M. Agio, "Silicon-vacancy color centers in phosphorus-doped diamond," Diamond Relat. Mater. **105**, 107797 (2020).
[27]K. K. Rebane, *Impurity Spectra of Solids: Elementary Theory of Vibrational Structure* (Springer, Boston, MA, 1995).
[28]A. M. Zaitsev, *Optical Properties of Diamond* (Springer, Berlin/Heidelberg, 2001).
[29]L. Bergman, M. T. McClure, J. T. Glass, and R. J. Nemanich, "The origin of the broadband luminescence and the effect of nitrogen doping on the optical properties of diamond films," J. Appl. Phys. **76**(5), 3020–3027 (1994).
[30]A. E. Mora, J. W. Steeds, and J. E. Butler, "Relationship between grain boundaries and broad luminescence peaks in CVD diamond films," Diamond Relat. Mater. **12**(3–7), 310–317 (2003).
[31]K. G. Lee, X. W. Chen, H. Eghlidi, P. Kukura, R. Lettow, A. Renn, V. Sandoghdar, and S. Götzinger, "A planar dielectric antenna for directional single-photon emission and near-unity collection efficiency," Nat. Photonics **5**(3), 166–169 (2011).
[32]H. Galal and M. Agio, "Highly efficient light extraction and directional emission from large refractive-index materials with a planar Yagi-Uda antenna," Opt. Mater. Express **7**(5), 1634 (2017).